

PCCP

Accepted Manuscript



This is an *Accepted Manuscript*, which has been through the Royal Society of Chemistry peer review process and has been accepted for publication.

Accepted Manuscripts are published online shortly after acceptance, before technical editing, formatting and proof reading. Using this free service, authors can make their results available to the community, in citable form, before we publish the edited article. We will replace this *Accepted Manuscript* with the edited and formatted *Advance Article* as soon as it is available.

You can find more information about *Accepted Manuscripts* in the [Information for Authors](#).

Please note that technical editing may introduce minor changes to the text and/or graphics, which may alter content. The journal's standard [Terms & Conditions](#) and the [Ethical guidelines](#) still apply. In no event shall the Royal Society of Chemistry be held responsible for any errors or omissions in this *Accepted Manuscript* or any consequences arising from the use of any information it contains.

Cite this: DOI: 10.1039/c0xx00000x

ARTICLE

www.rsc.org/xxxxxx

Thermal Vibration of a Single-walled Carbon Nanotube Predicted by Semiquantum Molecular Dynamics

Rumeng Liu^a, Lifeng Wang^{*a}

Received (in XXX, XXX) Xth XXXXXXXXX 20XX, Accepted Xth XXXXXXXXX 20XX

DOI: 10.1039/b000000x

Quantum effects should be considered in the thermal vibrations of carbon nanotubes (CNTs). To this end, a molecular dynamics based on modified Langevin dynamics, which accounts for quantum statistics by introducing a quantum heat bath, is used to simulate the thermal vibration of a cantilevered single-walled CNT (SWCNT). A nonlocal elastic Timoshenko beam model with quantum effects (TBQN), which can take the effect of microstructure into consideration, is established to explain the resulting power spectral density of the SWCNT. The root of mean squared (RMS) amplitude of the thermal vibration of the SWCNT obtained from the semiquantum molecular dynamics (SQMD) is lower than that obtained from the classical molecular dynamics, especially at very low temperature and high-order modes. The natural frequencies of the SWCNT obtained from the Timoshenko beam model are closer to those obtained from molecular dynamics if the nonlocal effect is taken into consideration. However, the nonlocal Timoshenko beam model with the law of energy equipartition (TBCN) can only predict the RMS amplitude of the SWCNT obtained from classical molecular dynamics without considering quantum effects. The RMS amplitude of the SWCNT obtained from the SQMD and that obtained from the TBQN coincide very well. These results indicate that quantum effects are important for the thermal vibration of the SWCNT in the case of high-order modes, short length and low temperature.

1. Introduction

Thermal fluctuations are very closely related with the resonance properties of low-dimensional structures as they serve as nanoscale devices¹⁻⁴. The thermal vibration problems of a carbon nanotube (CNT), which can be used as a nanoelectronic component^{5, 6} and AFM tip^{7, 8}, have attracted much research interest. Transmission electron microscopy is used to estimate the Young's modulus of the CNTs by measuring the amplitude of their intrinsic thermal vibrations^{9, 10}. Recently, Moser et al. studied CNT mechanical resonators at a cryostat temperature of 1.2 K and 30 mK using an ultrasensitive method based on cross-correlated electrical noise measurements, in combination with parametric downconversion^{11, 12}. In addition to experiment methods, molecular dynamics (MD) and continuum models¹³⁻¹⁹ are very important tools to study thermal vibration in CNTs.

However, in classical molecular dynamics (CMD), which does not allow for the description of quantum effects, each dynamical degree of freedom possesses the same average kinetic energy $k_B T/2$ at thermal equilibrium, where k_B is the Boltzmann constant and T is temperature. The pure quantum method is difficult to model in detail for the dynamics of many-body systems because of its complexity. However, some studies have shown that the quantum effects should be considered when the CNT vibrates at a low enough temperature^{20, 21}. To overcome these obstacles, different semi-classical methods, which can include quantum effects into the dynamics of nano-systems, have been proposed²²⁻²⁹. Dammak et al.²⁶ presented a semiquantum molecular dynamics (SQMD) that accounts for quantum statistics by introducing a quantum heat bath. In this approximation, both a dissipative force and a Gaussian random force having the power spectral density given by the quantum fluctuation-dissipation theorem³⁰ are introduced into a Langevin-type approach. Very recently, Wang and Hu³¹ studied the thermal vibration of a single-walled CNT (SWCNT) using classical beam theory with quantum effects taken into consideration instead of the law of energy equipartition. It shows that the root of mean squared (RMS) amplitude of thermal vibration of a SWCNT predicted by the quantum theory is lower than that predicted by the law of energy equipartition. However, the effect of the microstructure of SWCNTs, which has a significant influence on the vibrations and

^a State Key Laboratory of Mechanics and Control of Mechanical Structures,
Nanjing University of Aeronautics and Astronautics,
210016 Nanjing, PR China
Fax: +86 25 8489 2003-8004; Tel: +86 25 8489 2003-8004;
E-mail: walfe@nuaa.edu.cn

Cite this: DOI: 10.1039/c0xx00000x

www.rsc.org/xxxxxx

ARTICLE

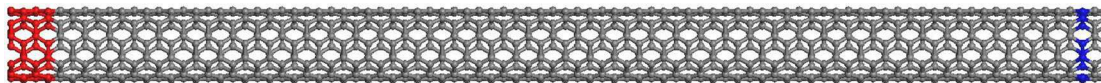


FIG. 1. Molecular structure model for an armchair (5, 5) SWCNT. Atoms in red are fixed, trajectories of the blue ones are recorded during simulations.

wave propagation of SWCNTs³², is not included in the beam models. In order to understand the influence of quantum effects to thermal vibrations of CNTs, a recent developed SQMD method is used to simulate free thermal vibration of a cantilevered SWCNT. The thermal vibrational spectrum of the SWCNT with quantum effects is presented first in this paper. Moreover, a nonlocal elastic beam theory with quantum effects taken into consideration is established to explain the resulting power spectral density of the SWCNT.

This paper is organized as follows. In Section 2, the SQMD method based on Langevin dynamics, which will be used to calculate the RMS amplitude spectrum, is presented. In Section 3, the nonlocal Timoshenko beam model with quantum effects is established. Section 4 outlines a comparison between the resulting power spectral density of the SWCNT calculated by SQMD and CMD. The natural frequency and RMS amplitude of thermal vibration of the SWCNT obtained from the nonlocal elastic Timoshenko beam model with quantum effects (TBQN) and the nonlocal Timoshenko beam model with the law of energy equipartition (TBCN) are listed for analysis. Finally, the paper ends with some conclusions in Section 5.

2. MOLECULAR DYNAMICS MODEL

Here, the CMD and the SQMD methods used to study thermal vibrations of SWCNTs are briefly presented. The dynamic equation of each atom in the molecular dynamics simulation is based on the Langevin equation. The dynamics equation of the n -th atom with mass M_n and position \mathbf{r}_n is

$$M_n \ddot{\mathbf{r}}_n = \mathbf{F}_n - M_n \gamma \dot{\mathbf{r}}_n + \mathbf{\Xi}_n, \quad (1)$$

where \mathbf{F}_n is the force caused by the interaction with all the other atoms, γ is the effective frictional coefficient, and $\mathbf{\Xi}_n = \{\xi_{\alpha n}\}_{\alpha=1}^3$ are random forces with the Gaussian distribution. In the CMD, $\mathbf{\Xi}_n$ and γ are related by the fluctuation-dissipation theorem at temperature T

$$\langle \xi_{\alpha n}(t) \xi_{\beta m}(0) \rangle = 2M_n \gamma k_B T \delta_{\alpha\beta} \delta_{nm} \delta(t), \quad (2)$$

where $\delta_{\alpha\beta}$ and δ_{nm} are the Kronecker symbol, while $\delta(t)$ is the Dirac delta function.

To include quantum features into molecular dynamics, for an oscillator with frequency ν at temperature T , the power spectral density of the random forces is given by the quantum fluctuation-dissipation theorem³⁰

$$\langle \xi_{\alpha n} \xi_{\beta m} \rangle_{\nu} = 2M_n \gamma k_B T \delta_{\alpha\beta} \delta_{nm} p(\nu, T), \quad (3)$$

where

$$p(\nu, T) = \frac{1}{2} \frac{\hbar \nu}{k_B T} + \frac{\hbar \nu / k_B T}{e^{(\hbar \nu / k_B T)} - 1}. \quad (4)$$

Different from the white noise generated by Equation (2) in CMD, the stochastic force spectrum is a color noise³³⁻³⁵. In this paper, a technique proposed by Savin *et al.*³⁵ is used to generate random forces.

The dimensionless power spectral density in Equation (4) can be expressed as

$$p(\bar{\nu}) = \frac{1}{2} \bar{\nu} + \frac{\bar{\nu}}{e^{\bar{\nu}} - 1}, \quad (5)$$

where $\bar{\nu} = \hbar \nu / k_B T$ is a dimensionless frequency.

The dimensionless random vector functions $\mathbf{S}_n(\tau) = \{S_{\alpha, n}\}_{\alpha=1}^3 = S_{0n}(\tau) + S_{1n}(\tau)$ of the dimensionless time $\tau = t k_B T / \hbar$ are constructed to generate the color noise. The power spectral density of random forces in Equation (3) is given as:

$$\langle \xi_{\alpha n} \xi_{\beta m} \rangle_{\nu} = 2M_n \gamma k_B T \langle S_{\alpha n} S_{\beta m} \rangle_{\bar{\nu}}, \quad (6)$$

and

$$\langle S_{\alpha n} S_{\beta m} \rangle_{\bar{\nu}} = \langle S_{0\alpha n} S_{0\beta m} \rangle_{\bar{\nu}} + \langle S_{1\alpha n} S_{1\beta m} \rangle_{\bar{\nu}}. \quad (7)$$

Here, the random functions $S_{0n}(\tau)$ and $S_{1n}(\tau)$ are uncorrelated,

and $S_{0n}(\tau)$ will generate the power spectra $\frac{1}{2} \bar{\nu}$, while $S_{1n}(\tau)$

will generate $\frac{\bar{\nu}}{e^{\bar{\nu}} - 1}$ in Equation (5). The first term in Equation

(7) gives the contribution of the zero-point oscillations to the power spectral density of random forces, and it does not need to be taken into account during the CNTs thermal-vibration simulations.

The random function $S_{1\alpha n}(\tau)$ can be approximated by a sum of two random functions with relatively narrow frequency spectra

$$S_{1\alpha n}(\tau) = c_1 \zeta_{\alpha n 1}(\tau) + c_2 \zeta_{\alpha n 2}(\tau). \quad (8)$$

In this sum, the dimensionless random functions $\zeta_{\alpha n i}(\tau)$, $i=1, 2$, satisfy the equations of motion as

$$\zeta_{\alpha n i}''(\tau) = \eta_{\alpha n i}(\tau) - \bar{\Omega}_i^2 \zeta_{\alpha n i}(\tau) - \bar{\Gamma}_i \zeta_{\alpha n i}'(\tau), \quad (9)$$

where $\eta_{\alpha n i}(\tau)$ are δ -correlated white-noise functions

$$\langle \eta_{\alpha n i}(\tau) \eta_{\beta k j}(\tau') \rangle = 2\bar{\Gamma}_i \delta_{\alpha\beta} \delta_{nk} \delta_{ij} \delta(\tau - \tau'), \quad (10)$$

where $c_1 = 1.8315$, $c_2 = 0.3429$, $\bar{\Omega}_1 = 2.7189$, $\bar{\Omega}_2 = 1.2223$,

$\bar{\Gamma}_1 = 5.0142$, $\bar{\Gamma}_2 = 3.2974$ are dimensionless parameters. $S_{\alpha n}(\tau)$

can be generated by solving numerically Equation (8),

$\mathbf{\Xi}_n = \{\xi_{\alpha, n}\}_{\alpha=1}^3$ in Equation (1) can be obtained by

$$\xi_{\alpha n}(t) = \xi_{\alpha n}(\hbar \tau / k_B T) = k_B T \sqrt{2M_n \gamma / \hbar} S_{1\alpha n}(\tau). \quad (11)$$

For a single-walled armchair (5, 5) CNT shown in Fig. 1, the first four rings of atoms at one end of the tube are fixed to simulate a cantilever boundary condition. To avoid the possible boundary effect of the last layer at the free end, the tip position u is the average position of the third last ring of 10 atoms. The molecular dynamics simulations are carried out based on Brenner's second-generation reactive empirical bond order (REBO) potential³⁶, which has been widely used in many studies on the mechanical behavior of carbon materials. The long-range van der Waals interaction is calculated by the Lennard-Jones 12-6 potential.³⁷ The velocity verlet formulation of the BBK integrator³⁸ with time step 1 fs is used during the simulations.

The canonical ensemble is often used as initial conditions for trajectories with constant energy dynamics^{18, 19} to calculate the RMS amplitude of the thermal vibration of the CNT. This method can be used for the case in which heat bath follows the law of equipartition. However, for the system in the color-noise heat bath, the energy will transfer from the low-frequency modes to the high-frequency ones in the micro-canonical ensemble³⁵. To avoid this problem, the systems are simulated by Langevin equations with very small friction coefficients for 10 ns at a constant temperature to generate thermal-equilibrium states. The tip displacement $u(t)$ is sampled at 10 fs intervals during the last 2 ns. The RMS amplitude spectrum of the free tip of the SWCNT is

$$u_{RMS}(v) = \frac{\sqrt{2}}{2} u(v), \quad (12)$$

where $u(v)$ is the Fourier transform of $u(t)$, and the one-sided spectrum type is selected during the transform. To increase the accuracy of the calculations, the final result is the averaging of 60 independent simulations.

3. NONLOCAL TIMOSHENKO BEAM WITH QUANTUM EFFECTS

To predict the mechanical behavior of CNTs with small-scale effects, nonlocal continuum theory, such as the nonlocal Timoshenko beam model has been widely used to study wave propagation and vibration of CNTs³⁹⁻⁴³. This section starts with the dynamic equations of a nonlocal Timoshenko beam of uniform cross-section with length L placed along direction x in the (x, y, z) coordinate system. The dynamic equations of the beam are

$$\rho A \left[1 - r_0^2 \frac{\partial^2}{\partial x^2} \right] \frac{\partial^2 w}{\partial t^2} + \beta AG \left(\frac{\partial \varphi}{\partial x} - \frac{\partial^2 w}{\partial x^2} \right) = 0, \quad (13a)$$

$$\rho I \left[1 - r_0^2 \frac{\partial^2}{\partial x^2} \right] \frac{\partial^2 \varphi}{\partial t^2} + \beta GA \left(\varphi - \frac{\partial w}{\partial x} \right) - EI \frac{\partial^2 \varphi}{\partial x^2} = 0, \quad (13b)$$

where $w(x, t)$ is the displacement of section x of the beam in direction y at the moment t , φ is the slope of the deflection curve of the beam when the shearing force is neglected, A is the cross section area of the beam, $I = \int y^2 dA$ is the moment of inertia for the cross section of the beam, β is the form factor of shear depending on the shape of the cross-section. E , ρ , G are Young's modulus, mass density and shear modulus of the beam, respectively. r_0 is a small-scale parameter with length unit describing effects of the microstructure on elastic behavior. In many research works, it has been revealed that the small-scale

effect is significant on wave propagation and thermal vibration in CNTs⁴⁴⁻⁴⁹. However, no experiments have been conducted to predict the magnitude of r_0 for CNTs. Wang and Hu obtained r_0 by a comparative study of the gradient method with atomic lattice dynamics and it yields³²

$$r_0 = \frac{d}{\sqrt{12}}, \quad (14)$$

where d is the axial distance between two particles in the materials. For the armchair SWCNT, d is the axial distance between two rings of carbon atoms.

The boundary conditions of a cantilever beam are

$$w(0, t) = 0, \quad \varphi(0, t) = 0, \quad \frac{\partial^2 w(L, t)}{\partial x^2} = 0, \quad \frac{\partial^2 \varphi(L, t)}{\partial x^2} = 0. \quad (15)$$

The dynamic deflection and slope can be given by

$$w = \hat{w} e^{j\omega t}, \quad \varphi = \hat{\varphi} e^{j\omega t}, \quad (16)$$

where \hat{w} represents the deflection amplitude of the beam, $\hat{\varphi}$ is the slope amplitude of the beam due to bending deformation alone, and $j = \sqrt{-1}$. Let

$$\xi = x / L. \quad (17)$$

Substituting Equations (16), (17) into Equation (13), one obtains

$$b^2 s^2 \hat{w} - L \frac{\partial \hat{\varphi}}{\partial \xi} + \frac{\partial^2 \hat{w}}{\partial \xi^2} - \frac{\rho r_0^2 \omega^2}{\beta G} \frac{\partial^2 \hat{w}}{\partial \xi^2} = 0, \quad (18a)$$

$$(b^2 r^2 s^2 - 1) \hat{\varphi} + \frac{1}{L} \frac{\partial \hat{w}}{\partial \xi} + s^2 \frac{\partial^2 \hat{\varphi}}{\partial \xi^2} - \frac{\rho I r_0^2 \omega^2}{L^2 \beta GA} \frac{\partial^2 \hat{\varphi}}{\partial \xi^2} = 0, \quad (18b)$$

where

$$b^2 = \frac{\rho A L^4 \omega^2}{EI}, \quad r^2 = \frac{I}{A L^2}, \quad s^2 = \frac{EI}{\beta A G L^2}. \quad (19)$$

Eliminating $\hat{\varphi}$, Equation (18) becomes

$$BC \frac{\partial^4 \hat{w}}{\partial \xi^4} + (BD + L^2 + b^2 s^2 C) \frac{\partial^2 \hat{w}}{\partial \xi^2} + b^2 s^2 D \hat{w} = 0, \quad (20)$$

where

$$\begin{aligned} B &= \left(1 - \frac{\rho r_0^2 \omega^2}{\beta G} \right) \\ C &= \left(L^2 s^2 - \frac{\rho I r_0^2 \omega^2}{\beta GA} \right) \\ D &= L^2 (b^2 r^2 s^2 - 1). \end{aligned} \quad (21)$$

In the case of

$$\frac{-(BD + L^2 + b^2 s^2 C) + \left[(BD + L^2 + b^2 s^2 C)^2 - 4BCD b^2 s^2 \right]^{1/2}}{2BC} \geq 0, \quad (22)$$

the solutions \hat{w} , $\hat{\varphi}$ of Equation (20) read⁵⁰

$$\hat{w} = C_1 \cosh \alpha_1 \xi + C_2 \sinh \alpha_1 \xi + C_3 \cos \alpha_2 \xi + C_4 \sin \alpha_2 \xi, \quad (22a)$$

$$\hat{\varphi} = C_1' \sinh \alpha_1 \xi + C_2' \cosh \alpha_1 \xi + C_3' \sin \alpha_2 \xi + C_4' \cos \alpha_2 \xi, \quad (22b)$$

where

$$\alpha_1 = \frac{1}{\sqrt{2BC}} \left\{ \mp (BD + L^2 + b^2 s^2 C) + \left[(BD + L^2 + b^2 s^2 C)^2 - 4BCD b^2 s^2 \right]^{1/2} \right\}, \quad (23)$$

In Equation (22), only one half of the constants are independent because they are related by Equation (18) as follows:

$$\left(b^2 s^2 + \left(1 - \frac{\rho r_0^2 \omega^2}{\beta G} \right) \alpha_1^2 \right) C_1 / (L \alpha_1) = C_1' = \Lambda_1 C_1, \quad (24a)$$

$$\left(b^2 s^2 + \left(1 - \frac{\rho r_0^2 \omega^2}{\beta G}\right) \alpha_1^2\right) C_2 / (L \alpha_1) = C_2' = \Lambda_1 C_2, \quad (24b)$$

$$\left(b^2 s^2 - \left(1 - \frac{\rho r_0^2 \omega^2}{\beta G}\right) \alpha_2^2\right) C_3 / (L \alpha_2) = C_3' = \Lambda_2 C_3, \quad (24c)$$

$$-\left(b^2 s^2 - \left(1 - \frac{\rho r_0^2 \omega^2}{\beta G}\right) \alpha_2^2\right) C_4 / (L \alpha_2) = C_4' = -\Lambda_2 C_4. \quad (24d)$$

The natural frequencies of the cantilever beam can be obtained by solving the following equation

$$\begin{vmatrix} 1 & 0 & 1 & 0 \\ 0 & \Lambda_1 & 0 & -\Lambda_2 \\ \alpha_1^2 \cosh \alpha_1 & \alpha_1^2 \sinh \alpha_1 & -\alpha_2^2 \cos \alpha_2 & -\alpha_2^2 \sin \alpha_2 \\ \alpha_1^2 \Lambda_1 \sinh \alpha_1 & \alpha_1^2 \Lambda_1 \cosh \alpha_1 & -\alpha_2^2 \Lambda_2 \sin \alpha_2 & \alpha_2^2 \Lambda_2 \cos \alpha_2 \end{vmatrix} = 0. \quad (25)$$

The natural modes (\hat{w}_n , $\hat{\phi}_n$) of the n -th order for the cantilever Timoshenko beam yield

$$\hat{w}_n = D_n f_{w_n}(\xi) = D_n \begin{bmatrix} \cosh \alpha_{n1} \xi + \frac{\Lambda_2}{\Lambda_1 \Lambda_3} \sinh \alpha_{n1} \xi \\ -\cos \alpha_{n2} \xi + \frac{1}{\Lambda_3} \sin \alpha_{n2} \xi \end{bmatrix}, \quad (26a)$$

$$\hat{\phi}_n = D_n f_{\phi_n}(\xi) = H_n \begin{bmatrix} \cosh \alpha_{n1} \xi - \frac{\Lambda_1}{\Lambda_2 \Lambda_4} \sinh \alpha_{n1} \xi \\ -\cos \alpha_{n2} \xi + \frac{1}{\Lambda_4} \sin \alpha_{n2} \xi \end{bmatrix}, \quad (26b)$$

where

$$\Lambda_3 = \frac{\left(-\frac{\Lambda_2}{\Lambda_1} \alpha_1^2 \sinh \alpha_1 + \alpha_2^2 \sin \alpha_2\right)}{\left(\alpha_1^2 \cosh \alpha_1 + \alpha_2^2 \cos \alpha_2\right)}, \quad (27a)$$

$$\Lambda_4 = -\frac{1}{\Lambda_3}, \quad (27b)$$

$$H_n = (\Lambda_2 / \Lambda_3) D_n. \quad (27c)$$

In the case of

$$\frac{-(BD + L^2 + b^2 s^2 C) + \left[(BD + L^2 + b^2 s^2 C)^2 - 4BCDB^2 s^2\right]^{1/2}}{2BC} < 0.$$

The solutions \hat{w} , $\hat{\phi}$ of Equation (20) read⁵⁰

$$\hat{w} = C_1 \cos \alpha_1' \xi + j C_2 \sin \alpha_1' \xi + C_3 \cos \alpha_2 \xi + C_4 \sin \alpha_2 \xi, \quad (28a)$$

$$\hat{\phi} = j C_1' \sin \alpha_1' \xi + C_2' \cos \alpha_1' \xi + C_3' \sin \alpha_2 \xi + C_4' \cos \alpha_2 \xi, \quad (28b)$$

where

$$\alpha_1' = \frac{1}{\sqrt{2BC}} \left\{ \frac{(BD + L^2 + b^2 s^2 C) - \left[(BD + L^2 + b^2 s^2 C)^2 - 4BCDB^2 s^2\right]^{1/2}}{2} \right\}^{1/2}. \quad (29)$$

Similar to Equation (22), in Equation (28), only half of the constants are independent,

$$\left(b^2 s^2 - \left(1 - \frac{\rho r_0^2 \omega^2}{\beta G}\right) \alpha_1'^2\right) / L j \alpha_1' C_1 = C_1' = \Lambda_1' C_1, \quad (30a)$$

$$-\left(b^2 s^2 j - \left(1 - \frac{\rho r_0^2 \omega^2}{\beta G}\right) j \alpha_1'^2\right) / L \alpha_1' C_2 = C_2' = \Lambda_2' C_2, \quad (30b)$$

$$\left(b^2 s^2 - \left(1 - \frac{\rho r_0^2 \omega^2}{\beta G}\right) \alpha_2^2\right) / L \alpha_2 C_3 = C_3' = \Lambda_3' C_3, \quad (30c)$$

$$-\left(b^2 s^2 - \left(1 - \frac{\rho r_0^2 \omega^2}{\beta G}\right) \alpha_2^2\right) / L \alpha_2 C_4 = C_4' = \Lambda_4' C_4. \quad (30d)$$

The natural frequencies of the cantilever beam yield the following equation:

$$\begin{vmatrix} 1 & 0 & 1 & 0 \\ 0 & \Lambda_1' & 0 & \Lambda_4' \\ \alpha_1'^2 \cos \alpha_1' & j \alpha_1'^2 \sin \alpha_1' & \alpha_2^2 \cos \alpha_2 & \alpha_2^2 \sin \alpha_2 \\ \Lambda_1' j \alpha_1'^2 \sin \alpha_1' & \Lambda_2' \alpha_1'^2 \cos \alpha_1' & \Lambda_3' \alpha_2^2 \sin \alpha_2 & \Lambda_4' \alpha_2^2 \cos \alpha_2 \end{vmatrix} = 0. \quad (31)$$

The natural modes (\hat{w}_n , $\hat{\phi}_n$) of the n -th order for the cantilever Timoshenko beam yield:

$$\hat{w}_n = D_n f_{w_n}(\xi) = D_n \begin{bmatrix} \cos \alpha_{n1}' \xi + j \frac{\Lambda_4'}{\Lambda_2' \Lambda_5'} \sin \alpha_{n1}' \xi \\ -\cos \alpha_{n2} \xi - \frac{1}{\Lambda_5'} \sin \alpha_{n2} \xi \end{bmatrix}, \quad (32a)$$

$$\hat{\phi}_n = D_n f_{\phi_n}(\xi) = H_n \begin{bmatrix} \cos \alpha_{n1}' \xi + j \frac{\Lambda_1'}{\Lambda_3' \Lambda_6'} \sin \alpha_{n1}' \xi \\ -\cos \alpha_{n2} \xi - \frac{1}{\Lambda_6'} \sin \alpha_{n2} \xi \end{bmatrix}, \quad (32b)$$

where

$$\Lambda_5' = \frac{\left(\alpha_2^2 \sin \alpha_2 - \frac{\Lambda_2'}{\Lambda_1'} j \alpha_1'^2 \sin \alpha_1'\right)}{\left(\alpha_1'^2 \cos \alpha_1' - \alpha_2^2 \cos \alpha_2\right)}, \quad (33a)$$

$$\Lambda_6' = \frac{\Lambda_4'}{\Lambda_5' \Lambda_3'}, \quad (33b)$$

$$H_n = (\Lambda_4' / \Lambda_5') D_n. \quad (33c)$$

The total energy E_n contained in the n -th vibration mode can be found by calculating the kinetic energy at the instant of equilibrium position of the beam

$$\begin{aligned} E_n &= \frac{1}{2} \int_0^L \left[\rho A \left(\frac{\partial w_n}{\partial t} \right)^2 + \rho I \left(\frac{\partial \phi_n}{\partial t} \right)^2 \right]_{t=\frac{\pi}{\omega_n}} dx + \\ &= \frac{1}{2} r_0^2 \int_0^L \left[\rho A \left(\frac{\partial^2 w_n}{\partial x \partial t} \right)^2 + \rho I \left(\frac{\partial^2 \phi_n}{\partial x \partial t} \right)^2 \right]_{t=\frac{\pi}{\omega_n}} dx \\ &= \frac{\rho L D_n^2 \omega_n^2}{2} \int_0^1 \left[A \left(f_{w_n}(\xi) \right)^2 + I \left(f_{\phi_n}(\xi) \right)^2 \right] d\xi + \\ &= \frac{\rho L D_n^2 \omega_n^2 r_0^2}{2 L^2} \int_0^1 \left[A \left(\frac{\partial f_{w_n}(\xi)}{\partial \xi} \right)^2 + I \left(\frac{\partial f_{\phi_n}(\xi)}{\partial \xi} \right)^2 \right] d\xi. \end{aligned} \quad (34)$$

The expression for mean energy contained in n -th vibration mode with quantum effects is^{31, 51}

$$\langle E \rangle = \frac{h \nu_n}{e^{h \nu_n / k_B T} - 1}, \quad (35)$$

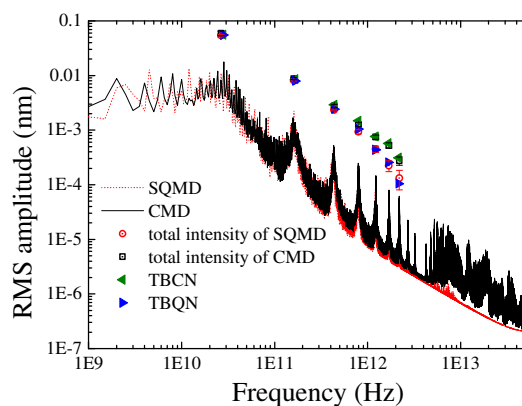
where $\nu_n = \omega_n / 2\pi$. The Boltzmann constant and the Planck's constant are $k_B = 1.38 \times 10^{-23} \text{ J K}^{-1}$, $h = 6.626 \times 10^{-34} \text{ J} \cdot \text{s}$, respectively.

Let the total energy in Equation (34) equal the mean energy in Equation (35), it is easily obtained

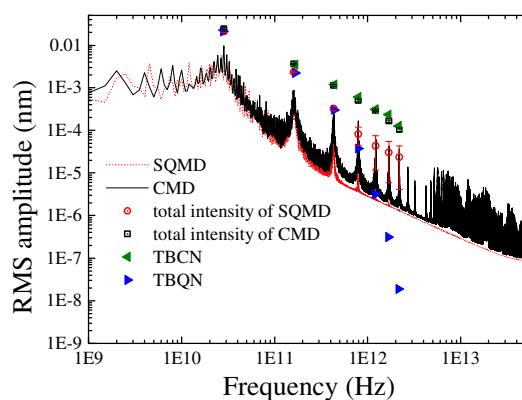
Cite this: DOI: 10.1039/c0xx00000x

ARTICLE

www.rsc.org/xxxxxx



(a)



(b)

FIG. 2. The thermal vibrational spectra for a 9.84 nm (5, 5) SWCNT at (a) $T=30\text{K}$ and (b) at $T=5\text{K}$.

Table 1. Frequencies (GHz) of (a) a 9.84 nm (5, 5) CNT at different temperatures predicted by beam theory and MD simulations.

N	TBCN/ TBQN $\beta = 0.6$	TBCN/ TBQN $\beta = 0.8$	CMD (300K)	SQMD (300K)	CMD (30K)	SQMD (30K)	CMD (5K)	SQMD (5K)
1	27.78	27.89	28.50	26.50	28.50	26.50	28.50	26.50
2	163.4	166.3	166.5	160.5	162.5	160.5	160.5	160.5
3	423.3	436.9	439.5	435.5	432.0	427.5	430.0	427.5
4	758.2	793.3	801.5	797.5	791.0	785.5	791.0	785.5
5	1143	1210	1229	1223	1219	1211	1217	1211
6	1561	1668	1699	1693	1691	1683	1689	1683
7	1999	2154	2191	2186	2190	2180	2185	2180

Table 2. RMS amplitude (nm) of (a) a 9.84nm (5, 5) CNT at different temperatures predicted by beam theory and MD simulations, where $\beta = 0.8$.

T	N	TBCN	TBQN	CMD	SQMD
300K	1	1.7687×10^{-1}	1.7667×10^{-1}	1.8457×10^{-1}	1.6563×10^{-1}
	2	2.7061×10^{-2}	2.6881×10^{-2}	2.7426×10^{-2}	2.6009×10^{-2}

	3	9.2135×10^{-3}	9.0530×10^{-3}	8.8051×10^{-3}	8.5099×10^{-3}
	4	4.7024×10^{-3}	4.5540×10^{-3}	4.0666×10^{-3}	4.0665×10^{-3}
	5	2.4120×10^{-3}	2.2962×10^{-3}	2.3652×10^{-3}	2.1466×10^{-3}
	6	1.8183×10^{-3}	1.6984×10^{-3}	1.3801×10^{-3}	1.2087×10^{-3}
	7	9.8717×10^{-4}	9.0346×10^{-4}	8.8298×10^{-4}	7.5817×10^{-4}
30K	1	5.5930×10^{-2}	5.5305×10^{-2}	5.8560×10^{-2}	5.4011×10^{-2}
	2	8.5573×10^{-3}	7.9948×10^{-3}	8.8158×10^{-3}	8.1759×10^{-3}
	3	2.9136×10^{-3}	2.4218×10^{-3}	2.7904×10^{-3}	2.3305×10^{-3}
	4	1.4870×10^{-3}	1.0474×10^{-3}	1.2791×10^{-3}	9.3402×10^{-4}
	5	7.6274×10^{-4}	4.3571×10^{-4}	7.4650×10^{-4}	4.5071×10^{-4}
	6	5.7501×10^{-4}	2.5640×10^{-4}	5.2534×10^{-4}	2.2357×10^{-4}
	7	3.1217×10^{-4}	1.0517×10^{-4}	2.7725×10^{-4}	1.3188×10^{-4}
5K	1	2.2833×10^{-2}	2.1317×10^{-2}	2.4481×10^{-2}	2.1172×10^{-2}
	2	3.4935×10^{-3}	2.2251×10^{-3}	3.6359×10^{-3}	2.3263×10^{-3}
	3	1.1895×10^{-3}	3.0155×10^{-4}	1.1309×10^{-3}	3.2326×10^{-4}
	4	6.0707×10^{-4}	3.7202×10^{-5}	5.0417×10^{-4}	8.1970×10^{-5}
	5	3.1139×10^{-4}	3.1829×10^{-6}	2.9253×10^{-4}	4.3226×10^{-5}
	6	2.3475×10^{-4}	3.1314×10^{-7}	1.6552×10^{-4}	3.0395×10^{-5}
	7	1.2744×10^{-4}	1.8800×10^{-8}	1.0432×10^{-4}	2.3644×10^{-5}

Table 3. Frequencies (GHz) of (a) a 19.68 nm (10, 10) CNT at different temperatures predicted by beam theory and MD simulations.

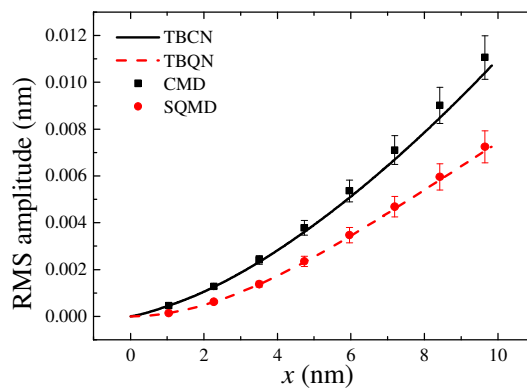
N	TBCN/ TBQN $\beta=0.6$	TBCN/ TBQN $\beta=0.8$	CMD (300K)	SQMD (300K)	CMD (30K)	SQMD (30K)
1	13.31	13.36	14.00	13.00	13.50	13.00
2	78.81	80.07	78.50	75.00	77.50	75.00
3	205.6	211.7	210.0	207.0	207.0	198.5
4	370.9	386.9	379.0	377.0	376.5	371.5
5	562.7	593.7	578.0	576.5	574.5	562.0
6	771.9	822.5	795.0	792.0	791.5	778.0
7	992.7	1066	1021	1018	1016	1004

Table 4. RMS amplitude (nm) of (a) a 19.68nm (10, 10) CNT at different temperatures predicted by beam theory and MD simulations,

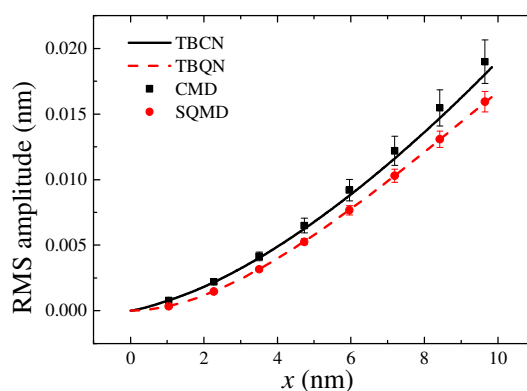
5

where $\beta=0.6$.

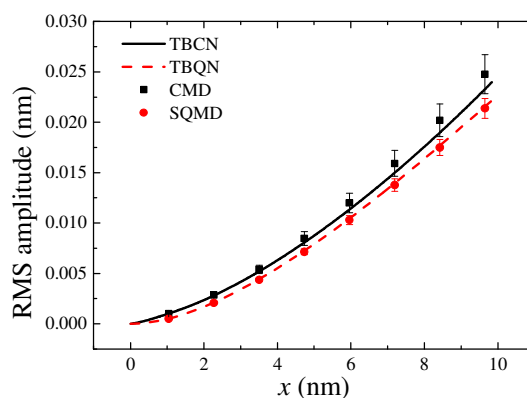
T	N	TBCN	TBQN	CMD	SQMD
300K	1	1.8767×10^{-1}	1.8757×10^{-1}	1.8870×10^{-1}	1.6833×10^{-1}
	2	2.9908×10^{-2}	2.9814×10^{-2}	2.8582×10^{-2}	2.8375×10^{-2}
	3	1.0556×10^{-2}	1.0469×10^{-2}	1.0429×10^{-2}	9.9678×10^{-3}
	4	5.6195×10^{-3}	5.5364×10^{-3}	5.0083×10^{-3}	5.0005×10^{-3}
	5	2.9976×10^{-3}	2.9304×10^{-3}	3.2253×10^{-3}	3.1182×10^{-3}
	6	2.3943×10^{-3}	2.3208×10^{-3}	2.0962×10^{-3}	1.9721×10^{-3}
	7	1.3511×10^{-3}	1.2979×10^{-3}	1.4386×10^{-3}	1.3520×10^{-3}
30K	1	5.9347×10^{-2}	5.9030×10^{-2}	5.9588×10^{-2}	5.7219×10^{-2}
	2	9.4579×10^{-3}	9.1609×10^{-3}	9.2849×10^{-3}	9.0482×10^{-3}
	3	3.3381×10^{-3}	3.0677×10^{-3}	3.7827×10^{-3}	2.8741×10^{-3}
	4	1.7771×10^{-3}	1.5208×10^{-3}	1.6963×10^{-3}	1.3802×10^{-3}
	5	9.4793×10^{-4}	7.4430×10^{-4}	9.9591×10^{-4}	7.4916×10^{-4}
	6	7.5715×10^{-4}	5.3887×10^{-4}	7.4592×10^{-4}	4.4723×10^{-4}
	7	4.2727×10^{-4}	2.7283×10^{-4}	4.5831×10^{-4}	3.6986×10^{-4}



(a)



(b)



(c)

FIG. 3. The RMS amplitude of a 9.84 nm (5, 5) SWCNT at (a) $T=1\text{K}$ (b) $T=3\text{K}$ and (c) $T=5\text{K}$.

$$D_n^2 = \frac{\frac{h\nu_n}{e^{h\nu_n/k_B T} - 1}}{\left\{ \frac{\rho L \omega_n^2}{2} \int_0^1 \left[A(f_{w_n}(\xi))^2 + I(f_{\varphi_n}(\xi))^2 \right] d\xi + \frac{\rho L \omega_n^2 r_0^2}{2 L^2} \int_0^1 \left[A\left(\frac{\partial f_{w_n}(\xi)}{\partial \xi}\right)^2 + I\left(\frac{\partial f_{\varphi_n}(\xi)}{\partial \xi}\right)^2 \right] d\xi \right\}} \quad (36)$$

$$D_n^2 = \frac{k_B T}{\left\{ \frac{\rho L \omega_n^2}{2} \int_0^1 \left[A(f_{w_n}(\xi))^2 + I(f_{\varphi_n}(\xi))^2 \right] d\xi + \frac{\rho L \omega_n^2 r_0^2}{2 L^2} \int_0^1 \left[A\left(\frac{\partial f_{w_n}(\xi)}{\partial \xi}\right)^2 + I\left(\frac{\partial f_{\varphi_n}(\xi)}{\partial \xi}\right)^2 \right] d\xi \right\}} \quad (37)$$

Then, the RMS amplitude of the thermal vibration of the n -th mode for the beam at x reads

¹⁰ For the case of $h\nu \ll k_B T$, Equation (36) becomes

$$\hat{w}_{RMS_n}(x) = \frac{\sqrt{2}}{2} D_n f_{w_n}(x). \quad (38)$$

As the natural modes are independent of one another, their contributions can be added incoherently. To average coherently over all the modes, the variances $\hat{w}_{RMS_n}^2(x)$ can be added to obtain the other Gaussian distribution with the standard deviation given by

$$\hat{w}_{RMS}(x) = \sqrt{\sum_{n=1}^{\infty} \hat{w}_{RMS_n}^2(x)}. \quad (39)$$

Hence, the RMS amplitude of thermal vibration of a SWCNT at any point can be obtained via the model of nonlocal Timoshenko beam model.

4. RESULTS AND DISCUSSION

Figures 2(a) and 2(b) show thermal vibrational spectra of a 9.84 nm armchair (5, 5) CNT at $T=30\text{K}$ and at $T=5\text{K}$, respectively. The solid line and dotted line are vibrational spectra calculated by CMD and SQMD methods, respectively. All spectra clearly have distinct peak, every distinct peak of the spectra represents one natural frequency of the SWCNT, and they are listed in Table 1. It shows that natural frequencies obtained by SQMD are very close to those obtained by CMD, which means quantum effects have little effect on the resonance frequency of SWCNT. Furthermore, Figure 2 shows that the RMS amplitude spectrum calculated by SQMD method is much lower than that calculated by CMD in the high-frequency range. The reason should be that the mean energy $\langle E \rangle$ of every vibrational mode in SQMD is much lower than that in CMD when the frequency is high enough. Thus, vibration of the high-frequency mode is frozen if the white noise is replaced by the color noise with quantum fluctuation-dissipation theorem.

To make a quantitative comparison of the Timoshenko beam theory with the MD results, it is necessary to know Young's modulus E and the shear modulus G or Poisson's ratio μ . The previous studies⁵² based on the REBO potential gave a great variety of Young's moduli and Poisson's ratios of SWCNTs. The molecular dynamics simulation of pure bending was carried out to obtain material parameters. The Young's modulus is $E=0.740$ TPa and the Poisson's ratio $\mu=0.254$ for the armchair (5, 5) SWCNTs, and $E=0.798$ TPa, $\mu=0.317$ for the armchair (10, 10) SWCNTs when the thickness of the SWCNTs was chosen as 0.34 nm.

Furthermore, Table 1 lists the frequencies obtained by Timoshenko beam theory. The shear coefficient β in the Timoshenko beam theory is related to the cross-section of the beam. In fact, the equivalent beam model of an armchair (5, 5) SWCNT is a thick-walled tube if the wall is chosen as 0.34 nm. Table 1 shows that the shear coefficient has a strong effect on high-order frequencies. By comparison with the results of the MD simulations, the Timoshenko beam models produce better predictions when the shear coefficient is taken as 0.8, which is close to the suggested value given by Cowper⁵³.

The total intensity of each spectrum peak corresponding to the RMS amplitude of thermal vibration of the SWCNT, can be calculated by summing the square of the RMS amplitude spectrum between the midpoints to the two adjacent peaks¹⁹. The RMS amplitude of the first seven modes is displayed in Figure 2.

It can be found that the RMS amplitude obtained by SQMD is lower than that obtained by CMD. Table 2 shows that the difference between the RMS amplitude obtained from these two MD methods becomes more obvious in the case of higher-order modes and lower temperatures. TBCN give good predictions for the RMS amplitude obtained from CMD. Furthermore, RMS amplitude obtained from TBQN are close to that obtained from SQMD.

The natural frequencies and RMS amplitude of the thermal vibrations of a 19.68 nm armchair (10, 10) SWCNT are shown in Table 3 and Table 4. Compared with the armchair (5, 5) SWCNT, the value of the wall thickness divided by the diameter becomes smaller. Table 3 shows that the Timoshenko beam models produce better predictions when the shear coefficient is taken as 0.6 for the armchair (10, 10) SWCNT. The RMS amplitude data listed in Table 2 and Table 4 shows that quantum effects have a greater effect on the SWCNT with smaller scale. For example, the seventh-order RMS amplitude of the (5, 5) SWCNT obtained by TBQN is 33.7% of that obtained by TBCN when the temperature is 30K. The corresponding value of the (10, 10) SWCNT is 63.9%. Moreover, some similar conclusions can be gotten by analyzing the RMS amplitude obtained from CMD and SQMD.

Figure 3 shows the RMS amplitude at different sections of a 9.84 nm long (5, 5) SWCNT at $T=5\text{K}$, $T=3\text{K}$ and $T=1\text{K}$. The RMS amplitude can be obtained by

$$\hat{w}_{RMS}(x) = \sqrt{\frac{\sum_{i=1}^N u_i^2(x)}{N}}, \quad (40)$$

where N is the total recorded steps of the molecular dynamics. As one can see from Figure 3, the difference between the CMD and SQMD methods becomes more significant at lower temperature. The RMS amplitude obtained from Timoshenko beam models gives the same tendency as well. These results means the quantum effect is more important for thermal vibration of the SWCNT at lower temperature.

For the difference between Timoshenko beam model and MD, the use of shear coefficient of Timoshenko beam may cause the error. More accurate models, such as higher-order shear deformation theory⁵⁴⁻⁵⁶ and shell model together with the quantum effect may give a better prediction to the natural frequency and RMS of CNTs.

5. CONCLUSIONS

In summary, a detailed study is herein presented on the thermal vibrations of cantilever SWCNTs using molecular dynamics with a quantum heat bath. The thermal vibrational spectrum of a SWCNT cantilever obtained from SQMD is much lower than that obtained from CMD. The natural frequency and RMS amplitude of thermal vibrations of the SWCNT obtained from the SQMD are very close to those obtained from TBQN. Nevertheless, the TBCN model can only give prediction for the results obtained by CMD. The results obtained from the CMD and SQMD methods indicate that quantum effects are important for the thermal vibrations of the SWCNTs in the case of high-order modes, small scale and low temperature.

ACKNOWLEDGEMENTS

This work was supported in part by the Foundation for the Author of the National Excellent Doctoral Dissertation of China under Grants 201028, Program for New Century Excellent Talents in University under Grants NCET-11-0832, the Funding for Outstanding Doctoral Dissertation in NUAA under Grants BCXJ13-03, Funding of Jiangsu Innovation Program for Graduate Education under Grants CXZZ13-0144 and in part by the Fundamental Research Funds for the Central Universities of China.

References:

- ¹ R. Ciocan, J. Gaillard, M. J. Skove, and A. M. Rao, *Nano Lett* **5**, 2389 (2005).
- ² P. Poncharal, Z. L. Wang, D. Ugarte, and W. A. de Heer, *Science*, 1999, **283**, 1513.
- ³ D. Garcia-Sanchez, A. San Paulo, M. Esplandiu, F. Perez-Murano, L. Forró, A. Aguasca, and A. Bachtold, *Phys Rev Lett*, 2007, **99**, 085501.
- ⁴ X. L. Wei, Y. Liu, Q. Chen, M. S. Wang, and L. M. Peng, *Adv Funct Mater*, 2008, **18**, 1555.
- ⁵ M. Ahlskog, P. Hakonen, M. Paalanen, L. Roschier, and R. Tarkiainen, *J Low Temp Phys*, 2001, **124**, 335.
- ⁶ L. Roschier, R. Tarkiainen, M. Ahlskog, M. Paalanen, and P. Hakonen, *Appl Phys Lett*, 2001, **78**, 3295.
- ⁷ M. Ishikawa, M. Yoshimura, and K. Ueda, *Appl Surf Sci*, 2002, **188**, 456.
- ⁸ E. S. Snow, P. M. Campbell, and J. P. Novak, *Appl Phys Lett*, 2002, **80**, 2002.
- ⁹ M. M. J. Treacy, T. W. Ebbesen, and J. M. Gibson, *Nature*, 1996, **381**, 678.
- ¹⁰ A. Krishnan, E. Dujardin, T. W. Ebbesen, P. N. Yianilos, and M. M. J. Treacy, *Phys Rev B*, 1998, **58**, 14013.
- ¹¹ J. Moser, J. Güttinger, A. Eichler, M. J. Esplandiu, D. E. Liu, M. I. Dykman and A. Bachtold, *Nat Nanotechnol*, 2013, **8**, 493.
- ¹² J. Moser, A. Eichler, J. Güttinger, M. I. Dykman and A. Bachtold, *Nat Nanotechnol*, 2014, **9**, 1007.
- ¹³ H. Jiang, Y. Huang, and K. C. Hwang, *J Eng Mater-T Asme*, 2005, **127**, 408.
- ¹⁴ A. W. Barnard, V. Sazonova, A. M. van der Zande, and P. L. McEuen, *P Natl Acad Sci USA*, 2012, **109**, 19093.
- ¹⁵ H. Jiang, B. Liu, Y. Huang, and K. C. Hwang, *J Eng Mater-T Asme*, 2004, **126**, 265.
- ¹⁶ L. F. Wang, H. Y. Hu, and W. L. Guo, *P Roy Soc A-Math Phy*, 2010, **466**, 2325.
- ¹⁷ L. F. Wang and H. Y. Hu, *Acta Mech*, 2012, **223**, 2107.
- ¹⁸ E. H. Feng and R. E. Jones, *Phys Rev B*, 2011, **83**, 195412.
- ¹⁹ E. H. Feng and R. E. Jones, *Phys Rev B*, 2010, **81**, 125436.
- ²⁰ J. Hone, B. Batlogg, Z. Benes, A. T. Johnson, and J. E. Fischer, *Science*, 2000, **289**, 1730.
- ²¹ J. Zimmermann, P. Pavone, and G. Cuniberti, *Phys Rev B*, 2008, **78**, 045410.
- ²² C. Y. Li and T. W. Chou, *Phys Rev B*, 2005, **71**, 075409.
- ²³ S. Buyukdagli, A. V. Savin, and B. B. Hu, *Phys Rev E*, 2008, **78**, 066702.
- ²⁴ J. S. Wang, X. X. Ni, and J. W. Jiang, *Phys Rev B*, 2009, **80**, 224302.
- ²⁵ M. Ceriotti, G. Bussi, and M. Parrinello, *Phys Rev Lett*, 2009, **103**, 030603.
- ²⁶ H. Dammak, Y. Chalopin, M. Laroche, M. Hayoun, and J. J. Greffet, *Phys Rev Lett*, 2009, **103**, 190601.
- ²⁷ J. S. Wang, *Phys Rev Lett*, 2007, **99**, 160601.
- ²⁸ E. M. Heatwole and O. V. Prezhdo, *J Phys Soc Jpn*, 2008, **77**, 044001.
- ²⁹ D. Donadio and G. Galli, *Phys Rev Lett*, 2009, **103**, 255502.
- ³⁰ B. H. Callen and T. A. Welton, *Phys. Rev.*, 1951, **83**, 34.
- ³¹ L. F. Wang and H. Y. Hu, *P Roy Soc A-Math Phy*, 2014, **470**, 2168.
- ³² L. F. Wang and H. Y. Hu, *Phys Rev B*, 2005, **71**, 195412.
- ³³ A. A. Maradudin and T. Michel, *Ann Phys-New York*, 1990, **203**, 255.
- ³⁴ J. L. Barrat and D. Rodney, *J Stat Phys*, 2011, **144**, 679.
- ³⁵ A. V. Savin, Y. A. Kosevich, and A. Cantarero, *Phys Rev B*, 2012, **86**, 064305.
- ³⁶ D. W. Brenner, O. A. Shenderova, J. A. Harrison, S. J. Stuart, B. Ni, and S. B. Sinnott, *J Phys-Condens Mat*, 2002, **14**, 783.
- ³⁷ J. E. Jones, *P Roy Soc A-Math Phy*, 1924, **106**, 463.
- ³⁸ A. Brünger, C. L. Brooks III, and M. Karplus, *Chem. Phys. Letters*, 1984, **105**, 495.
- ³⁹ H. M. Berrabah, A. Tounsi, A. Semmah, and E. A. A. Bedia, *Struct Eng Mech*, 2013, **48**, 351.
- ⁴⁰ Y. Gafour, M. Zidour, A. Tounsi, H. Heireche, and A. Semmah, *Physica E*, 2013, **48**, 118.
- ⁴¹ H. Heireche, A. Tounsi, A. Benzair, and I. Mechab, *J. Appl. Phys*, 2008, **104**, 014301.
- ⁴² A. Tounsi, H. Heireche, H. M. Berrabah, A. Benzair, and L. Boumia, *J. Appl. Phys*, 2008, **104**, 104301.
- ⁴³ M. Zidour, K. H. Benrahou, A. Semmah, M. Naceri, H. A. Belhadj, K. Bakhti, and A. Tounsi, *Comp Mater Sci*, **51**, 252.
- ⁴⁴ H. Heireche, A. Tounsi, A. Benzair, M. Maachou, and E. A. A. Bedia, *Physica E*, 2008, **40**, 2791.
- ⁴⁵ A. Tounsi, A. Semmah, and A. A. Bousahla, *J. Micromech. Microeng*, 2013, **3**, 20.
- ⁴⁶ H. Heireche, A. Tounsi, and A. Benzair, *Nanotechnology*, 2008, **19**, 185703.
- ⁴⁷ S. Benguediab, A. Tounsi, M. Zidour, and A. Semmah, *Compos Part B-Eng*, 2014, **57**, 21.
- ⁴⁸ A. Benzair, A. Tounsi, A. Besseghier, H. Heireche, N. Moulay, and L. Boumia, *J. Phys. D. Appl. Phys*, 2008, **41**, 225404.
- ⁴⁹ K. Amara, A. Tounsi, I. Mechab, and E. Adda-Bedia, *Appl Math Model*, 2010, **34**, 3933.
- ⁵⁰ T. C. Huang, *J Appl Mech*, 1961, **28**, 579.
- ⁵¹ A. Lahiri, *Statistical mechanics: an elementary outline* (Universities Press (India) Private Ltd, 2009).
- ⁵² K. M. Liew, Y. Hu, and X. Q. He, *J Comput Theor Nanos*, 2008, **5**, 581.
- ⁵³ G. R. Cowper, *J Appl Mech*, 1966, **12**, 335.
- ⁵⁴ L. O. Larbi, A. Kaci, M. S. A. Houari, and A. Tounsi, *Mech Based Des Struc*, 2013, **41**, 421.
- ⁵⁵ M. Simsek, *Nucl Eng Des*, 2010, **240**, 697.
- ⁵⁶ Q. Wang and K. M. Liew, *Phys Lett A*, 2007, **363**, 236.